Observation of Nonlinear Optical Interactions of Ultralow Levels of Light in a Tapered Optical Nanofiber Embedded in a Hot Rubidium Vapor

S. M. Spillane,[1] G. S. Pati,[2] K. Salit,[2] M. Hall,[2] P. Kumar,[2] R. G. Beausoleil,[1] and M. S. Shahriar[2]

[1]*Hewlett-Packard Laboratories, Palo Alto, California 94304, USA*

[2]*Department of EECS, Northwestern University, Evanston, Illinois 60208, USA*

(Received 13 December 2007; published 11 June 2008)

We report the observation of low-light level optical interactions in a tapered optical nanofiber (TNF) embedded in a hot rubidium vapor. The small optical mode area plays a significant role in the optical properties of the hot vapor Rb-TNF system, allowing nonlinear optical interactions with nW level powers even in the presence of transit-time dephasing rates much larger than the intrinsic linewidth. We demonstrate nonlinear absorption and V-type electromagnetically induced transparency with cw powers below 10 nW, comparable to the best results in any Rb-optical waveguide system. The good performance and flexibility of the Rb-TNF system makes it a very promising candidate for ultralow power resonant nonlinear optical applications.

DOI: 10.1103/PhysRevLett.100.233602 PACS numbers: 42.50.Gy, 42.81.Qb

The interaction of light with atomic ensembles [1–3] has created a number of advancements in generating and controlling classical and quantum states of light [4–6]. In order to enable optical interactions with few photons (as desired in some quantum information processing studies [7]), much effort has been invested into increasing the interaction between atoms and photons. This is often done by employing high finesse optical microcavities, where quantum effects are readily observed between a single atom and a single photon [8–11]. However, these systems are extremely complicated. For applications where single-photon interactions are not needed, atomic ensembles in a simple nonresonant geometry are used to observe quantum optic effects. Previously, most work was performed with optical beams focused into an alkali vapor, where the use of a bulk, free-space geometry fundamentally limited the interaction strength and/or length [6]. Recent experiments have resulted in significant increases in both interaction strength and interaction length by encasing an atomic vapor into a waveguide [12,13], with V-system electromagnetically induced transparency (EIT) demonstrated in a photonic crystal fiber (PCF) with approximately 3 nW of pulsed power [12]. In both of these cases, the enhanced interaction comes from reducing the optical mode area. Here we explore the use of tapered optical nanofibers (TNF) with optical mode areas smaller than in previous experiments, and demonstrate low light level nonlinear interactions with a rubidium atomic vapor.

A TNF consists of a single-mode silica optical fiber where the original fiber diameter is reduced to the submicron range. In this system, the optical mode which was initially guided by the core (cladding) interface is adiabatically converted with negligible loss [14] into a mode guided by the cladding (environment) interface. The evanescent field extends into the surrounding environment, which for the purposes of this work consists of a rubidium atom vapor. The use of an evanescent interaction maintains the benefit of independently controlling the interaction strength (through cross-sectional geometry) and length (due to the invariance of the evanescent field along the waveguide), and allows an increase of interaction strength over previous waveguide approaches [12,13]. This system has been previously used to study evanescent interactions with Cs atoms, such as probing atom fluorescence [15,16]. In principle the interaction length can be arbitrary long, just as in any waveguide, with a limit due to intrinsic optical waveguide loss. For a TNF of diameter 400 nm, approximately 10% of the optical field interacts with the rubidium vapor. For this diameter, we estimate that the total number of atoms interacting with the TNF as 1400/cm, which for the typical taper length of 3 mm in this work gives a total number of atoms of ≈ 450 (assuming a Rb atomic density of 6×10^{12} atoms/cm^3 for a vapor at 100 °C).

We have investigated numerically the performance of the Rb-TNF system for different TNF geometries. Figure 1 shows a plot of the fraction of the optical energy located in the evanescent field and the optical mode area for a TNF versus diameter for an optical wavelength of 780 nm, corresponding to the Rb D_2 manifold. We see that as the diameter decreases the fraction of the optical energy that extends into the external Rb vapor increases monotonically. The optical mode area decreases as the diameter decreases to about 0.45 μm due to the added dielectric confinement, corresponding to a minimum optical mode area of 0.18 μm^2. As the diameter is reduced further, the mode quickly delocalizes, causing a rise in mode area. This minimum mode area is significantly smaller than that found in alternate waveguiding geometries ($>10\times$ smaller than antiresonant reflecting optical waveguides [13] and $>100\times$ smaller than PCF waveguides [12]), and is comparable to the atomic scattering cross section of $3\lambda^2/2\pi$. Therefore, we expect that the TNF should have a dramatically increased interaction with an atomic vapor.

However, in an open environment such as the Rb-TNF system, this mode area is so miniscule that a single atom

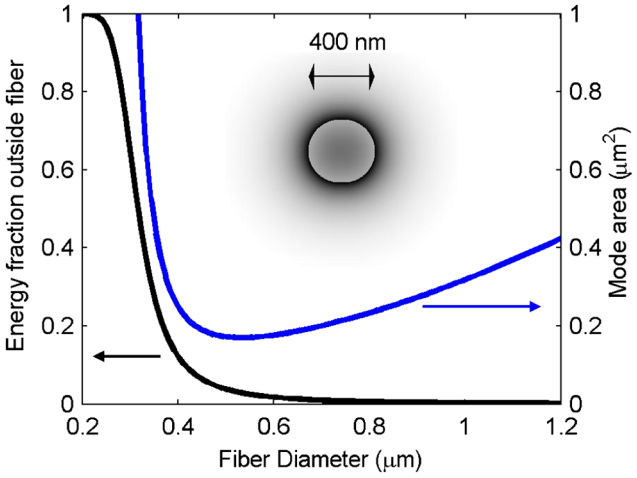

FIG. 1 (color online). Calculated mode area and external energy fraction for a TNF ($\lambda = 780$ nm). The inset shows the electric field distribution for the fundamental mode of a 400 nm diameter TNF.

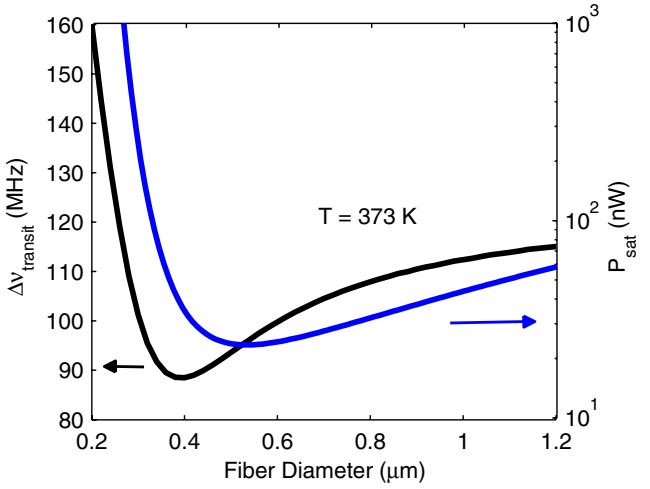

FIG. 2 (color online). Calculated transit-time linewidth and saturation power for a hot rubidium vapor (vapor temperature of 100 °C) coupled to a TNF. The saturation calculation assumes an intrinsic saturation intensity of 1.5 mW/cm^2 and a Doppler width of 575 MHz for the bulk vapor.

(with a velocity typically found in a hot vapor cell) passes through the optical field of the TNF in a few nanoseconds. This time is much shorter than the intrinsic decay time of the atom ($\approx$25 ns), leading to an effect known as transit-time broadening. Fundamentally, transit-time broadening can be understood by considering the optical interaction in the atom's reference frame. Here, the stationary atom experiences a temporally varying optical field, with a temporal shape dependent on the transverse optical mode field. In this case, the optical absorption linewidth is given by a combination of the intrinsic atomic decay rate and the transit-time decay rate (determined from the Fourier transform of the time-varying optical field), leading to a broader absorption line when transit-time effects dominate. Additionally, the presence of transit-time broadening can significantly increase the threshold to observe nonlinear interactions. Figure 2 shows a calculation of the transit-time dephasing rate expected for a Rb vapor interacting with a TNF of various diameters. For this calculation we used the exact TNF optical field profile to determine the dephasing rate for an atom passing through the evanescent field, assuming an isotropic angular distribution and that the atoms which struck the TNF bounced off with no delay and without dephasing (this gives an estimate of the smallest transit-time linewidth possible). This procedure was performed for all possible atomic speeds, with the final linewidth determined by integrating over a Maxwell-Boltzmann velocity distribution for a vapor with a temperature of 100 °C. The calculation shows that dephasing rates are on the order of 100 MHz, which is much larger than the intrinsic atom linewidth ($\approx$6 MHz), with a minimum value of 89 MHz for a TNF diameter of 400 nm.

An easy way to describe the suitability of a system for nonlinear optical effects is to consider the power needed to saturate an atomic vapor. This is given by the relation $P_{\mathrm{sat}} = I_{\mathrm{sat}} A_m (\gamma_T/\gamma_0)^2$, where I_{sat} is the saturation intensity for an atomic transition, A_m is the optical mode area, and γ_T/γ_0 represents the ratio of the total linewidth (including transit-time dephasing and Doppler broadening) and the intrinsic linewidth. Figure 2 shows the calculated nonlinear saturation power as a function of diameter corresponding to an isotropic Rb vapor of 100 °C, with $I_{\mathrm{sat}} =$ 1.5 mW/cm^2 for the D_2 manifold. In this case the Doppler width of 575 MHz is much larger than transit-time dephasing, so that the calculated saturation power is effectively independent of transit time. The data show that due to the small mode area the nonlinear saturation power is on the order of tens of nanowatts even in the presence of significant Doppler broadening.

In our experimental setup [Fig. 3(a)], a TNF was inserted into a chamber containing hot rubidium vapor, which contained a natural mixture of Rb^{85} and Rb^{87} isotopes. A Newport single-mode fiber at 780 nm was drawn adiabatically into a TNF with a waist diameter of approximately 400 nm using the "flame-brush" technique [17] with a hydrogen-air torch. The resulting taper profile is nearly exponential with a $1/e$ length of $\approx$3 mm. During the adiabatic tapering process, monitoring of fiber transmission showed negligible loss (ranging from 1%–10%) for final taper waist diameters of approximately 400 nm. The TNF is mounted to a copper chuck using UV-curable epoxy and inserted into the vacuum chamber using a set of Teflon fiber feedthroughs [18], which maintain fiber continuity into and out of the vacuum chamber. A gate valve isolates the optical fiber during loading or unloading from a rubidium metal source. During experiments, the vacuum chamber was heated to $\approx$100 °C (to minimize Rb condensation), and Rb vapor was created by heating the source region to $\approx$ 200 °C, with the chamber pressure maintained at 5 mTorr by a roughing pump. For these measurements, we made no attempt to prevent dephasing for atoms which

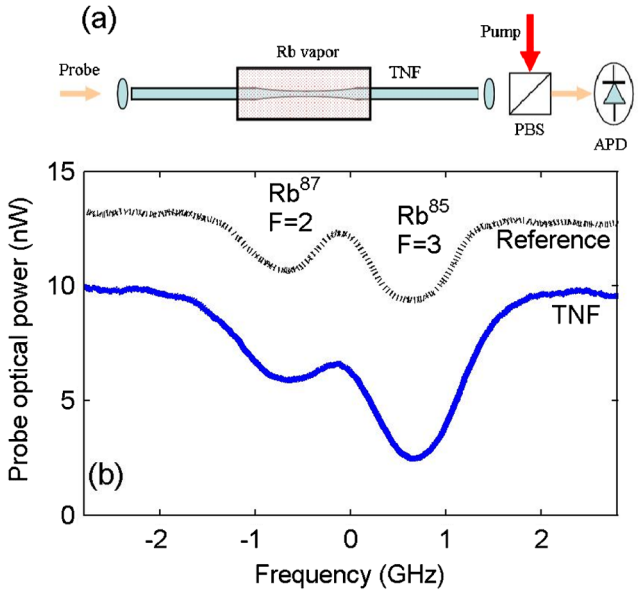

FIG. 3 (color online). (a) Diagram of the experimental setup. The tapered nanofiber passes through the Rb vapor-containing chamber using Teflon fiber feedthroughs. A polarization beam splitter is used to inject a strong counterpropagating cross-polarized pump for the saturated absorption and EIT measurements. (b) Transmitted spectrum for a TNF and reference cell for the D_2 manifold of Rb vapor at 780 nm.

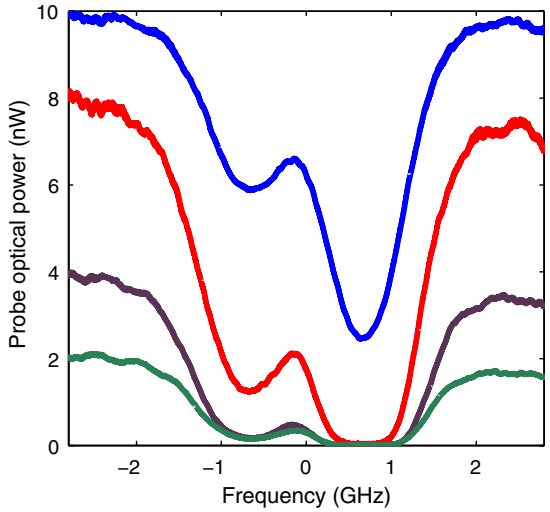

FIG. 4 (color online). Transmission spectrum for a TNF for increasing probe powers of {2, 4, 8, 10}nW for the Rb D_2 transition. The spectra show optical saturation with a saturation power of ≈ 8 nW.

struck the TNF. Assuming the vapor inside the chamber is at an average temperature of 100 °C, the atomic density is estimated to be $6 \times 10^{12}/\mathrm{cm}^3$.

For the first set of experiments, a weak probe beam (approximately 10 nW) obtained from a Ti:sapphire laser was transmitted through the TNF, and the optical transmission was monitored with an avalanche photodiode. The frequency of the probe was scanned over the Doppler broadened spectrum of the D_2 manifold. Figure 3(b) shows the transmission spectrum through the TNF (lower spectrum), and a reference Rb vapor cell kept at 100 °C (upper spectrum). The dip on the left corresponds to the $F = 2$ to $F' = 2$ transition in the D_2 manifold of Rb^{87}, while the dip on the right corresponds to the $F = 3$ to $F' = 3$ transition in the same manifold of Rb^{85}. Far away from resonance, the probe was found to be attenuated by about 20% due to a combination of losses at the input couplers and by TNF absorption. The data clearly show transmission dips representative of rubidium vapor absorption, with peak locations similar to that of the reference cell. However, the shape of the transmission dips for the Rb-TNF system is slightly different than that for the reference cell, which is due to both differences in Doppler broadening and transit-time dephasing present in this experimental measurement.

In optical saturation, the nonlinear absorption coefficient $\alpha_{\mathrm{NL}} = \alpha_0/(1 + P/P_{\mathrm{sat}})$, where α_0 is the linear absorption coefficient and P is the incident optical power. As the incident optical power increases in a nonlinear medium, the relative absorption decreases, and therefore the relative transmission increases. Figure 4 shows the transmitted power spectrum measured for a variety of incident power levels for a TNF with a waist diameter of approximately 400 nm. On the left edge, the output power is close to its value observed far away from resonance. The bottom (green) trace corresponds to an off-resonant, output probe power of about 2 nW. At this power level, the probe is found to be absorbed very strongly. As the probe power is increased, the relative transmission increases, as expected for a nonlinear medium. The absorption decrease with incident power can be used to extract the saturation power, which is approximately 8 nW. This value is lower than the theoretical value which we attribute to a nonisotropic atomic vapor in our experiment. Assuming an effective Doppler width of 210 MHz (inferred from measurements described below), we obtain a predicted saturation power of 4 nW. Accounting for the TNF profile, the saturation power increases to $\approx$ 8 nW, in good agreement with the measurement.

Next, a pump-probe measurement was performed, with the strong counterpropagating pump beam cross-polarized with respect to the probe. This measurement was performed on the D_1 manifold in order to delineate more clearly the spectral features in the presence of large transit-time broadening. Figure 5 illustrates the probe transmission spectrum (power $\approx$ 1 nW) for counterpropagating pump powers of 10 nW (middle, green) and 30 nW (lower, red), for a TNF with a waist diameter of approximately 400 nm. For comparison, a reference trace is also shown for a conventional vapor cell (upper, blue). The peaks on the left and the right correspond to self-induced transparency (SIT) for Rb^{85} atoms with zero axial velocities, corresponding to the $F = 3 - F' = 2$ and the $F = 3 - F' = 3$ hyperfine transitions, respectively. This measurement is similar to that of conventional saturated absorption spectroscopy, with a V-type three level EIT peak

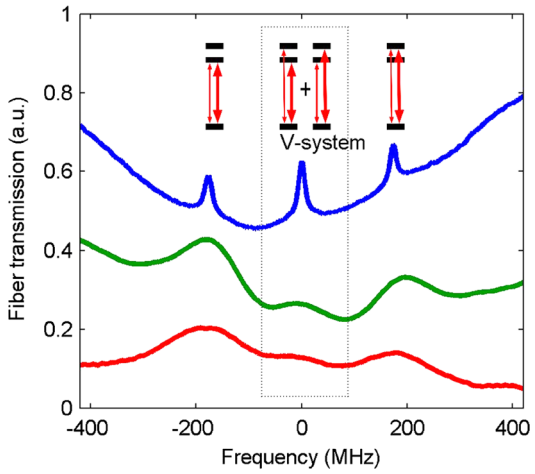

FIG. 5 (color online). Saturated absorption spectrum with cross-polarized pump and probe beams for a Rb vapor cell (upper, blue) and a Rb-TNF system (middle, green and lower, red) for the D_1 manifold of Rb^{85}. The two side peaks correspond to the Doppler-free $F = 3 - F' = 2$ and $F = 3 - F' = 3$ hyperfine lines, which are composed of atoms with near zero longitudinal velocity. These widths indicate the power-broadened hyperfine linewidth, including transit-time dephasing. The center peak corresponds to V-system EIT.

(with orthogonally polarized pump and probe) located at the crossover resonance location. This peak is composed of V-type EIT measurements of two groups of atoms (illustrated in Fig. 5): (a) one with an axial velocity such that the probe excites the $F = 3 - F' = 3$ transition and the pump excites the $F = 3 - F' = 2$ transition, and (b) the other with an equal but opposite axial velocity so that the probe excites the $F = 2 - F' = 3$ transition and the pump excites the $F = 3 - F' = 2$ transition. The EIT signal for the TNF is readily apparent for the lower pump power measurement, where the peak is clearly separated from the SIT peaks. The amplitude of this peak is measurably greater than the background signal for both the low and high power spectra, even though the high power spectrum is less resolvable due to power broadening.

For the conventional vapor cell, the transparency seen at the EIT resonance is larger than that at the SIT peaks due to the larger number of atoms in the combined ± 180 MHz Doppler-shifted groups (there is approximately 1.5 times the number of atoms in an isotropic vapor cell, which arises from the 575 MHz width of the Doppler distribution) than the individual zero axial velocity groups. Furthermore, the peak widths are the power-broadened individual hyperfine transitions (≈ 6 MHz power broadened to ≈ 18 MHz). However, for the TNF signal, there is a noticeable difference between the linewidths and relative amplitudes of the SIT and EIT peaks. Here, the line broadening for the lower (middle) power curve is due primarily to the transit-time effect. The transit-time broadening is about 110 MHz, close to the theoretical prediction. The dramatically smaller amplitude of the V-system EIT peak in the TNF measurement is likely due to a nonisotropic atomic velocity distribution in the Rb-TNF cell, which leads to a smaller population of atoms with the correct longitudinal Doppler-shifted velocity component for the EIT interaction. The relative magnitude of the three absorption peaks is consistent with a 210 MHz wide effective Doppler distribution, which also gives good agreement with the saturation power data in Fig. 4. The effective reduction of the Doppler width may be attributable to the geometry of the cell and the relative position of the TNF and the vacuum pump. Further investigation will be carried out in the future to study this effect.

In conclusion, we have shown that a TNF coupled to a Rb vapor exhibits optical saturation and EIT at very low pump power levels below 10 nW, comparable to the best results in any Rb-waveguide system. Numerical modeling indicates that the TNF's small mode area results in a significant linewidth broadening due to the short transit time of hot Rb atoms through the evanescent field, which combined with Doppler broadening increases the threshold for nonlinear optical effects. However, this is a limitation of the large atomic velocities in a high temperature Rb vapor, which can be reduced in principle. In particular, the use of cooled atoms from a magneto-optic trap [15,16] will allow the elimination of transit time and Doppler broadening, which should lead to nonlinear interactions with pW level optical powers.

This work was supported in part by the Hewlett-Packard Co. through DARPA and the Air Force Office of Scientific Research under AFOSR Contract No. FA9550-07-C-0030, and by AFOSR Grant No. FA9550-04-1-0189.

[1] S. E. Harris, Phys. Today **50**, No. 7, 36 (1997).
[2] M. D. Lukin, Rev. Mod. Phys. **75**, 457 (2003).
[3] M. Fleischhauer, A. Imamoglu, and J. P. Marangos, Rev. Mod. Phys. **77**, 633 (2005).
[4] S. E. Harris and Y. Yamamoto, Phys. Rev. Lett. **81**, 3611 (1998).
[5] M. C. Dawes *et al.*, Science **308**, 672 (2005).
[6] D. A. Braje *et al.*, Phys. Rev. A **68**, 041801(R) (2003).
[7] R. G. Beausoleil *et al.*, J. Mod. Opt. **51**, 2441 (2004).
[8] C. J. Hood *et al.*, Phys. Rev. Lett. **80**, 4157 (1998).
[9] C. J. Hood *et al.*, Science **287**, 1447 (2000).
[10] S. M. Spillane *et al.*, Phys. Rev. A **71**, 013817 (2005).
[11] T. Aoki *et al.*, Nature (London) **443**, 671 (2006).
[12] S. Ghosh *et al.*, Phys. Rev. Lett. **97**, 023603 (2006).
[13] W. Yang *et al.*, Nat. Photon. **1**, 331 (2007).
[14] G. Brambilla, V. Finazzi, and D. J. Richardson, Opt. Express **12**, 2258 (2004).
[15] K. P. Nayak *et al.*, Opt. Express **15**, 5431 (2007).
[16] G. Sague *et al.*, Phys. Rev. Lett. **99**, 163602 (2007).
[17] T. A. Birks and Y. W. Li, J. Lightwave Technol. **10**, 432 (1992).
[18] E. R. I. Abraham and E. A. Cornell, Appl. Opt. **37**, 1762 (1998).